



1 **Large-scale isotopic fingerprinting of cryosphere and hydrological**
2 **components in glacierized catchments**

3

4 Melanie Vital¹, Edison Jara¹, Andrew John Wade², Janie Masse-Dufresne³, Aurel Persoiu^{4,5,6},
5 Marjan Temovski⁷, Zarina Saidaliyeva⁸, Polona Vreča⁹, Luzmila Dávila Roller¹⁰, Maria
6 Shahgedanova², Tao Pu¹¹, Francisco Fernandoy¹², Lee Jeonghoon¹³, Bakhriddin Nishonov¹⁴,
7 Edson Ramirez¹⁵, Yuliya Vystavna¹.

8

9 *Correspondence to: Melanie Vital (m.vital@iaea.org)*

10 ¹Isotope Hydrology Section, Division of Physical and Chemical Sciences, Department of Nuclear Sciences
11 and Applications, International Atomic Energy Agency, Vienna International Centre, Wagramer Strasse 5,
12 1400 Vienna, Austria (M.Vital@iaea.org, e.jara-tarazona@iaea.org, Y.Vystavna@iaea.org)

13 ²The University of Reading, School of Archaeology, Geography and Environmental Science (SAGES), Walker
14 Institute for Climate System Research, Reading, United Kingdom (m.shahgedanova@reading.ac.uk,
15 a.j.wade@reading.ac.uk)

16 ³Université du Québec, École de technologie supérieure, Montréal, Canada (janie.masse-dufresne@etsmtl.ca)

17 ⁴Emil Racoviță Institute of Speleology, Romanian Academy, Cluj-Napoca, 400006, Romania
18 (aurel.persoiu@gmail.com)

19 ⁵Stable Isotope Laboratory, Ștefan cel Mare University, Suceava, 720229, Romania

20 ⁶School of Geology, Department of Physical Geography, Aristotle University of Thessaloniki, Thessaloniki,
21 54636, Greece

22 ⁷Isotope Climatology and Environmental Research Centre (ICER), HUN-REN Institute for Nuclear Research
23 (ATOMKI), Debrecen, Hungary, - Department of Mineralogy and Geology, University of Debrecen, Hungary
24 (temovski.marjan@atomki.hu)

25 ⁸Central Asian Regional Glaciological Centre under the auspices of UNESCO, Almaty, 050010, Kazakhstan
26 (z.saidaliyeva@outlook.com)

27 ⁹Department of Environmental Sciences, Jožef Stefan Institute, Jamova cesta 39, 1000 Ljubljana, Slovenia
28 (polona.vreca@ijs.si)

29 ¹⁰Instituto Nacional de investigación en glaciares y ecosistemas de montaña, Huaraz, Peru
30 (ldavila@inaigem.gob.pe)

31 ¹¹Northwest Institute of Eco-Environment and Resources, Chinese Academy of Sciences, Lanzhou, China
32 (putao@lzb.ac.cn)

33 ¹²Universidad Andrés Bello, Dept. Ciencias de la Tierra, Facultad de Ingeniería, Viña del Mar, Chile
34 (francisco.fernandoy@unab.cl)

35 ¹³Ewha Womans University, Dept. of Science Education, Seoul, Republic of Korea
36 (jeonghoon.lee@ewha.ac.kr)

37 ¹⁴Hydrometeorological Research Institute, Agency of Hydrometeorological Service of the Republic of
38 Uzbekistan, Tashkent, Uzbekistan (bnishonov@mail.ru)

39 ¹⁵Universidad Mayor de San Andrés, Instituto de Hidráulica e Hidrología, La Paz, Bolivia
40 (eramirez.umsa@gmail.com)

41
42



43 **Abstract.** Stable water isotopes (SWI; $\delta^{18}\text{O}$ and $\delta^2\text{H}$) are widely used tracers for identifying water
44 sources and reconstructing hydroclimatic processes in glacierized catchments. However, globally
45 harmonized isotope datasets that integrate multiple cryosphere and hydrological endmembers
46 remain limited. Here we present a global georeferenced database of stable water isotope
47 measurements compiled across glacierized catchments worldwide. The dataset contains 12,348
48 individual $\delta^{18}\text{O}$ and $\delta^2\text{H}$ measurements collected from 63 publications, covering 19 countries
49 across six continents. The temporal coverage of the isotope measurements spans from 1978
50 to 2023, based on data compiled from publications starting in 1981. The database integrates
51 isotope measurements from precipitation, snowpack and snowmelt, glacier ice, firn, glacial and
52 supraglacial meltwater, rock glaciers, ice-cored moraines, permafrost thaw waters, talus slopes,
53 streams, lakes, and groundwater. Each record includes standardized metadata describing
54 geographic location, elevation, sampling period, endmember classification, and analytical
55 methods. Across the compiled dataset, $\delta^{18}\text{O}$ values range from approximately -31‰ to -0.36‰ ,
56 while $\delta^2\text{H}$ values range from -247‰ to 0‰ , reflecting strong variability in elevation, temperature,
57 and moisture source conditions across glacierized environments. Cryosphere endmembers such
58 as glacier ice and glacial meltwater typically exhibit depleted signatures ($\delta^{18}\text{O} \approx -14\text{‰}$; $\delta^2\text{H} \approx$
59 -100‰) reflecting precipitation formed under colder climatic conditions and preserved within
60 glacier storage, while groundwater and firn waters tend to show relatively enriched compositions
61 due to mixing, recharge processes, and seasonal precipitation inputs. By harmonizing isotope
62 observations across multiple cryosphere and hydrological components, this database provides a
63 new global reference for identifying characteristic isotopic signatures of glacier-derived waters
64 and their downstream mixing with other hydrological sources. The dataset supports comparative
65 studies of glacier–hydrology interactions, endmember mixing analysis, and isotope-enabled
66 hydrological modelling, contributing to improved understanding of water resources in glacier-fed
67 catchments under changing climate conditions. The dataset is publicly available at
68 <https://doi.org/10.5281/zenodo.19062383> (Vital et al., 2026).

69

70 **1. Introduction**

71 Glaciers act as long-term freshwater reservoirs, help regulate seasonal river flows, and are
72 sensitive indicators of climate change (Huss et al., 2018; Clason et al., 2023). In many mountai
73 n regions, glacier melt sustains river discharge during dry and warm periods, supports downstream
74 ecosystems and provide water supplies to communities. Also, glaciers buffer hydrological



75 extremes by moderating both low-flow conditions and peak runoff (Millet et al., 2012; Laurent et
76 al., 2020; Slemmons et al., 2013; Viviroli et al., 2020).

77 Glacierized regions are unevenly distributed across the globe, with the largest glacierized areas
78 found in high-latitude environments and major mountain belts (RGI 7.0 Consortium, 2023). The
79 world's largest glacierized region outside the polar ice sheets is situated in High Mountain Asia,
80 including the Himalaya, Karakoram, and Hindu Kush which together store vast volumes of ice and
81 sustain major river systems (Clason et al., 2023). Additional glacierized systems occur in Central
82 Asia, Pamir, and Tien Shan, which are commonly treated as separate glacier regions due to their
83 distinct tectonic setting and continental climate regime. Other major glacierized regions include
84 the Arctic and sub-Arctic of North America (Alaska and the Canadian Arctic), the Andes of South
85 America, the Patagonian Ice fields, the European Alps, the Southern Alps of New Zealand, and the
86 high mountains of the Caucasus and the Altai and Sayan mountain systems (Li et al., 2023).

87 Although Antarctica and Greenland represent 40% of the global glacier ice volume (Li et al., 2023),
88 their hydrological settings differ from mountain catchments. In mountain catchments, meltwater
89 is typically routed through well-defined pathways, flowing over (supraglacial), through (englacial)
90 and beneath (subglacial) glaciers and seasonal snowpacks into proglacial streams, and
91 subsequently into river networks (Sharp and Tranter, 2017). Along this transit, a significant
92 fraction of meltwater may also infiltrate into the shallow subsurface, where it can be temporarily
93 stored in soils, talus slopes, moraines, or fractured bedrock, either in liquid or solid form,
94 contributing to shallow groundwater and delayed baseflow (Glas et al., 2018; Gordon et al., 2015).

95 In contrast, in polar environments, surface drainage networks are often sparse, discontinuous,
96 absent or are draining directly towards the surrounding oceans, with restricted contribution to
97 terrestrial hydrologic cycles (e.g., Perçoiu et al., 2023). For this reason, this study focuses on
98 glacierized systems at the continental scale where glaciers interact directly with surface waters
99 and groundwater.

100 Glaciers respond directly to variations in air temperature and precipitation through changes in
101 accumulation and melt and their evolution reflects the integrated effects of climatic forcing over
102 timescales ranging from seasons to decades (Thompson et al., 2003). In this context, stable water
103 isotopes (SWI) are natural constituents of the water molecule that can be used as tracers for
104 reconstructing past and present hydroclimatic conditions (Yoshimura, 2015; Dee et al., 2023, Kim,
105 2025). Stable oxygen and hydrogen isotopes in the water molecule ($\delta^{18}\text{O}$ and $\delta^2\text{H}$) record
106 information on moisture sources, elevation and temperature controls on glacier accumulation



107 and ablation, and post-depositional modification of precipitation signals, all of which are essential
108 for understanding the functioning of glacierized catchments. Moreover, SWI enable the
109 quantitative separation of cryosphere and hydrological contributions to streamflow (Wanner et
110 al., 2023; Dee et al., 2023; Müller et al., 2025; Evans, 2025). Consequently, integrating SWI analysis
111 into studies of glacierized catchments can be used to assess how glacier-derived water resources
112 are likely to evolve in response to ongoing climate change. This study presents the first global
113 compilation of SWI data from diverse hydrological components that represent cryosphere in
114 catchments, including the diversity of endmembers: precipitation, stream, lakes, groundwater,
115 snowpack, snow melt, glacial meltwater, supraglacial meltwater, firn, glacier ice, ice-core
116 moraines, rock glacier, permafrost thaw, and talus slopes. While $\delta^{18}\text{O}$ and $\delta^2\text{H}$ have been
117 extensively determined in individual components of the hydrosphere (e.g. Penna et al., 2014,
118 Chen et al., 2024), through global monitoring networks such as GNIP and GNIR (Craig, 1961;
119 Rozanski et al., 1993; Vitvar et al., 2007, IAEA/WMO, 2025), and in regional studies (e.g., Taylor et
120 al., 2001; Vreča et al., 2006, Vodila et al., 2011; Rets et al., 2019; Zhe et al., 2022; Lin et al., 2024,
121 Saidaliyeva et al., 2024; Chen et al., 2024a; Bai et al., 2025; Avesani et al., 2025; Nguyen et al.,
122 2025; Li et al., 2025a, 2025b), a comprehensive, harmonized dataset integrating cryosphere,
123 surface, and subsurface waters at the global scale has not previously been available.

124 The novelty of this work lies in its integration of multiple cryosphere and hydrological components
125 into a single georeferenced database that covers the spatial distribution of the cryosphere in
126 inhabited regions. This approach enables direct comparison of SWI signatures across
127 endmembers, continents, and climate regimes, revealing fractionation patterns and regionally
128 specific deviations driven by climate, elevation, and hydrological processes (Dansgaard, 1964;
129 Rozanski et al., 1993; Bojar, 2021; IAEA, 2022, Zhe et al., 2022). The database (Vital et al., 2026)
130 supports a wide range of applications, including: aid in selection of appropriate secondary
131 standards to cover the anticipated range in isotope ratio when making measurements on samples
132 from new field sites; isotope-based hydrograph separation and endmember mixing analysis
133 (Christophersen & Hooper, 1992; Kendall & McDonnell, 1998; He, 2019; Arora, 2024; Dar, 2024;
134 Muller, 2025); calibration and evaluation of isotope-enabled hydrological models in glacierized
135 catchments (Ala-aho et al., 2017; Bowen et al., 2019; IAEA 2025), estimation of transit time
136 (Staudinger et al., 2020) and the development of data-driven and artificial intelligence (AI) -based
137 predictive models of water balance and cryosphere–hydrology interactions. Further, by using
138 spatial distribution of SWI signatures in different endmembers in different climates as a proxy for



139 climate variability, it allows for a better understanding of their dynamics in response to past
140 processes and thus robust prediction for their future response to ongoing climatic changes (Vuille
141 et al., 2020; Vystavna et al., 2021, 2024).

142

143 2. Data and Methods

144 2.1. Endmembers definitions

145 In hydrology and geochemistry, endmembers represent the pure or unmixed water sources that
146 contribute to a mixture (Christophersen & Hooper 1992). Endmembers are idealized source of
147 water at the boundaries of the mixing space. Table 1 provides a definition for each endmember
148 used in this study, including precipitation, stream, lakes, groundwater, snowpack, snowpack melt,
149 glacial meltwater, supraglacial meltwater, firn, glacier ice, ice-core moraines, rock glacier,
150 permafrost thaw, and talus slopes.

151

152 *Table 1. Definitions and key references for hydrological and cryosphere endmembers included in*
153 *the isotope database in glacierized catchments.*

Endmembers	Definition	References
Precipitation	Meteoric water, including liquid, solid and mixed precipitation, isotopic composition governed by temperature, humidity, and source, following the Global Meteoric Water Line (GMWL).	Craig, 1961; Dansgaard, 1964
Stream	Integrates contributions from precipitation, snow, glacier melt, and groundwater.	Kendall and Coplen, 2001
Lakes	Reservoir water under open-water evaporative conditions. Its isotopic composition commonly shows enrichment along an evaporation line controlled by humidity wind and temperature	Gibson et al., 2002; Horita et al., 2008
Groundwater	Subsurface water integrating multiple recharge events over time; well mixed, isotopic values are damped relative to precipitation, indicative of recharge conditions, pattern and timing.	Clark and Fritz, 1997; Jasechko, 2017
Snowpack	Seasonally accumulated snow stored on the ground prior to melting. Snowpack isotopic composition integrates mainly winter precipitation signals and may be modified by sublimation, wind redistribution, summer rain events and melt-refreeze cycles.	Clark and Fritz., 1997; Taylor et al., 2001



Snowpack melt	Seasonal meltwater from snowpacks, often with lower $\delta^{18}\text{O}$ and $\delta^2\text{H}$ values compared to rainwater; key source of runoff in cold and mountain basins.	Taylor et al., 2001; Penna et al., 2014
Glacier meltwater	Meltwater derived from glacier ice; with lower $\delta^{18}\text{O}$ and $\delta^2\text{H}$ values compared to the stream water and precipitation due to sourcing from accumulation of cold-season precipitation and/or relict ice formed in past colder climates.	Jansson et al., 2003; Immerzeel et al., 2010
Supraglacial meltwater	Liquid water on the surface of a glacier, formed by the melting of snow and ice.	Müller et al., 2025
Glacier ice	Solid glacial mass formed from accumulated and compacted snow through firnification. Its meltwater represents a primary cryosphere endmember, typically depleted in heavy isotopes due to elevation effects, temperature-dependent fractionation, and Rayleigh distillation during snowfall.	Dansgaard, 1964
Firn	Partially compacted old snow, intermediate between snow and glacier ice in terms of density.	Ala-aho et al., 2017
Ice cored moraines	Morainic deposits that contain buried glacier ice beneath a cover of debris. Meltwater derived from ice-cored moraines typically reflects glacier ice isotopic signatures but may be altered by partial refreezing of meltwater within the moraine body.	Humlum, 2000
Rock glacier	Distinct bodies of a perennially frozen debris–ice mixture covered by a seasonally thawed debris layer.	Amschwand et al., 2025
Permafrost thaw	Water released during the thawing of previously frozen ground (permafrost), including ice-rich soil, ground ice, and buried glacier ice. Its isotopic composition reflects the original meteoric water preserved at the time of freezing, modified by freezing and thawing processes.	Woo, 2012
Talus slopes	Liquid water draining from coarse, steep debris accumulations at the base of cliffs or valley walls. Talus-slope waters often reflect rapid infiltration of snowmelt or precipitation with limited mixing, and in cold regions may include meltwater from interstitial ice or seasonal frozen ground.	Curry et al., 2023



154

155 **2.2. Data collection and Data quality**

156 The database contains 12,348 individual entries describing the isotopic signatures of hydrological
157 endmembers obtained from 63 publications. The list of publications used to build this database is
158 available in Supplementary material (Table S1). The database only includes single data; averages
159 of isotopic values are not included in this study. It extends to all inhabited continents, with
160 coverage across 20 countries and multiple climatic regions. The temporal coverage extends from
161 1981 to most recent publications (up to 2025). Peer-reviewed publications were identified
162 through systematic searches in major scientific databases, primarily Web of Science and Scopus.
163 Keyword combinations included “stable water isotopes”, “glacier meltwater”, “snowmelt
164 isotopes”, “cryosphere hydrology”, “glacierized catchments”, “ $\delta^{18}\text{O}$ ”, and “ $\delta^2\text{H}$ ”. In addition to
165 published sources, the database also integrates non-published isotope datasets collected directly
166 by the authors of this study. Each record includes 44 fields grouped into four categories:
167 bibliographic metadata (data owner, publication year, citation, published status); geographical
168 metadata (continent, country, catchment, glacier name, basin, coordinates); sampling details
169 (sample type, number of samples, sampling period, elevation, remarks); and stable isotope data
170 ($\delta^{18}\text{O}$, $\delta^2\text{H}$, d-excess, method, error, uncertainty) and sources (references). Endmember labels
171 were standardized to a controlled vocabulary used in endmember mixing analysis (EMMA). The
172 data were reported in $\delta^{18}\text{O}$ and $\delta^2\text{H}$ relative to VSMOW/VSMOW2 with units in per mil (‰). The
173 deuterium-excess (d-excess) was reported or calculated as $\delta^2\text{H} - 8 \cdot \delta^{18}\text{O}$ (Dansgaard, 1964).
174 Reported measurement techniques include isotope ratio mass spectrometry (IRMS) and laser
175 spectroscopy (Cavity Ring-Down Spectroscopy – CRDS and Off-Axis Integrated Cavity Output
176 Spectroscopy – OA-ICOS). The analytical methods reported for $\delta^{18}\text{O}$ measurements include CRDS:
177 9,192; IRMS: 2,738; OA-ICOS: 418. The same distribution applies to $\delta^2\text{H}$ analyses. The mean
178 reported one-sigma analytical uncertainties are approximately 0.13‰ for $\delta^{18}\text{O}$ and 0.49‰ for
179 $\delta^2\text{H}$. Outliers were flagged rather than removed for $\delta^{18}\text{O}$ values outside $[-40, +20]$ ‰, for $\delta^2\text{H}$
180 values outside $[-320, +120]$ ‰. Values of deuterium excess outside the range $[+0, +25]$ ‰ were
181 carefully flagged for further verification. While most precipitation globally exhibits d-excess values
182 close to +10 ‰, unusually high values may occur in cryosphere environments. Elevated d-excess
183 can result from kinetic fractionation processes associated with sublimation and vapor exchange
184 in snowpacks, glacier surfaces, and supraglacial environments, particularly under conditions of
185 low relative humidity and strong wind. Post-depositional modification of snow and ice may also



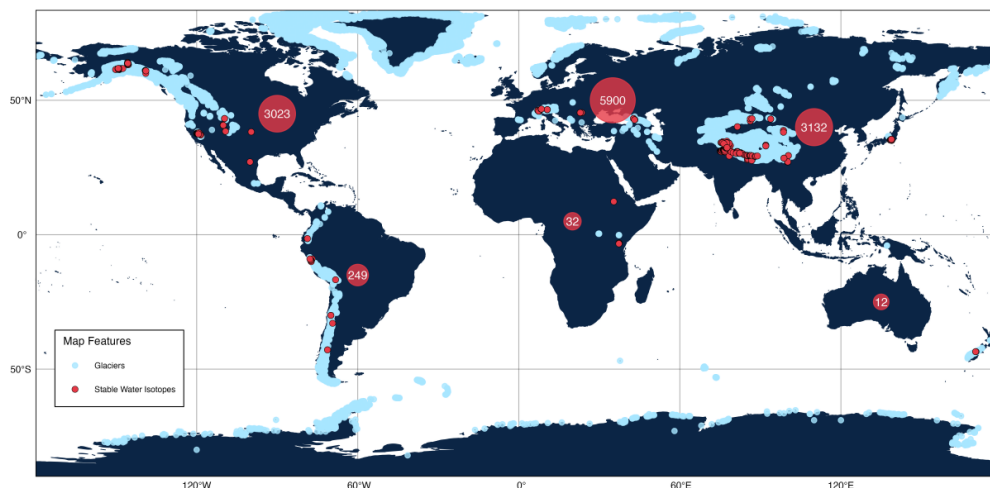
186 alter the original isotopic signal. In addition, extremely high values may occasionally reflect
187 analytical artefacts or transcription errors in the original sources. Flagging these records therefore
188 allows potentially modified or uncertain measurements to be identified while retaining them in
189 the dataset for transparency.

190

191 **2.3. Data distribution**

192 The isotope records are mostly clustered in Europe, particularly in the Alpine region (Fig. 1).
193 Additional major clusters occur in Asia, particularly in China and the broader High-Mountain Asia
194 domain, and in western North America, including Alaska, the Canadian Rockies, and mountainous
195 regions of the United States. Smaller clusters are present in the Andes of South America and in
196 selected sites in East Africa. Coverage in Oceania and other parts of Africa remains sparse. Overall,
197 the database comprises 12,348 records distributed across 20 countries and six continents: Europe
198 (5,899), Asia (3,132), North America (3,022), South America (249), Africa (32), and Oceania (12).
199 The catchments included in this study are concentrated in mountain regions outside the major
200 polar ice sheets: Asia, South America, and Europe together represent 75.0% of the study
201 catchments (28.1%, 26.6%, and 20.3%, respectively), despite accounting for only ~33% of global
202 glacier ice volume (Table 2). North America contributes 18.8% of the catchments, broadly
203 consistent with its large global share of glacier area and volume.

204



205

206 *Figure 1. Global map showing the geographic distribution of glacierized continental catchments*
207 *outside the major polar ice sheets included in the isotope endmember database. Red markers*



208 *indicate individual study locations, while red circles represent regional clustering with the number*
209 *of records compiled per region. This study focuses on glacierized systems at the continental scale*
210 *where glaciers interact directly with surface waters and groundwater.*

211

212 *Table 2. Regional distribution of glacier area and ice volume derived from Li et al. (2023), compared*
213 *with the number and proportion of glacierized catchments included in the isotope database. The*
214 *table summarizes global glacier area (km² and %), global ice volume (km³ and %), and the*
215 *representation of study catchments by region, highlighting the spatial coverage of isotopic*
216 *observations relative to global cryosphere distribution.*

217

Region	Global area (km ²)	Global area (%)	Global ice volume (km ³)	Global ice volume (%)	Number of catchments in this study (n)	catchments (%)
Africa	5	<0.1	0.2	<0.1	1	1.6
Asia	152915	21.7	25249	16.3	18	28.1
Europe	50060	7.1	11025	7.1	13	20.3
North America	247251	35.0	51593	33.2	12	18.8
South America	31760	4.5	6117	3.9	17	26.6
Oceania	1164	0.2	72	0.1	3	4.7

218

219 **3. Uncertainty, challenges and limitations in the construction of isotope** 220 **datasets**

221 Uncertainty is an inherent component of any large-scale environmental dataset, particularly when
222 it integrates measurements originating from multiple studies, laboratories, and sampling
223 contexts. In the present compilation of stable water isotope records from glacierized catchments,
224 uncertainty arises from several sources, including analytical precision of isotope measurements,
225 natural environmental variability, heterogeneity in sampling strategies, and limitations associated
226 with the integration and harmonization of datasets from diverse publications. Rather than
227 representing a single numerical value, uncertainty in this database should be understood as the
228 combined effect of these factors, which influence the interpretation and comparability of isotope
229 data across spatial and temporal scales.

230

231 **3.1. Uncertainty related to analytical precision**



232 A first level of uncertainty relates to analytical precision in the measurement of stable water
233 isotopes ($\delta^2\text{H}$ and $\delta^{18}\text{O}$). Most measurements included in this dataset were originally generated
234 using isotope ratio mass spectrometry (IRMS) or cavity ring-down spectroscopy (CRDS), both
235 widely used techniques in isotope hydrology. Under standard laboratory conditions, these
236 analytical systems typically achieve precisions on the order of $\pm 0.1\text{‰}$ for $\delta^{18}\text{O}$ and $\pm 0.5\text{--}1.0\text{‰}$ for
237 $\delta^2\text{H}$. Calibration procedures generally rely on internationally recognized reference materials,
238 including Vienna Standard Mean Ocean Water (VSMOW2), Standard Light Antarctic Precipitation
239 (SLAP2), ensuring comparability between laboratories operating within the international isotope
240 measurement framework. However, the dataset compiles results produced over several decades
241 and across many analytical facilities, meaning that reported precision may vary slightly depending
242 on instrument configuration, laboratory calibration procedures, and the analytical protocols
243 applied at the time of measurement. Where available, information on analytical precision
244 reported in the original publications was retained in the metadata, although such information was
245 not consistently provided across all studies. Elevated d-excess allows to flag uncertainty in
246 analytical precision, analytical artefacts, or transcription errors in the original sources.

247

248 **3.2. Uncertainty related to environmental variability**

249 Beyond laboratory precision, a significant component of uncertainty arises from environmental
250 variability and hydrological processes that influence isotope compositions in glacierized
251 catchments. Stable isotope signatures of water reflect integrated atmospheric and hydrological
252 processes including condensation history, temperature conditions during precipitation formation,
253 evaporation, sublimation, and mixing of different water sources. In glacierized environments,
254 additional processes such as snow metamorphism, meltwater refreezing, supraglacial
255 evaporation, and subglacial water storage can further modify isotope signatures. As a result,
256 differences observed between samples are not necessarily indicative of analytical error but rather
257 represent natural variability within the hydrological system. For instance, precipitation samples
258 may represent individual storm events, daily collections, or monthly composite samples
259 depending on the monitoring network. Similarly, glacier meltwater samples may represent
260 instantaneous stream samples, integrated catchment discharge, or localized supraglacial melt.
261 These differences introduce variability in isotope values that reflects real hydrological
262 heterogeneity rather than measurement uncertainty alone.

263



264 **3.3. Variability related to temporal sampling**

265 Temporal sampling differences also contribute to variability within the dataset. Some records
266 represent long-term monitoring programs spanning multiple years, while others correspond to
267 short field campaigns or isolated sampling events. Seasonal processes are particularly important
268 in glacierized basins, where isotope compositions can vary substantially between winter snow
269 accumulation, spring snowmelt, and late-summer glacier melt contributions. Consequently,
270 comparisons among studies should consider the temporal context of sampling, as differences in
271 seasonality can influence the isotopic composition of measured water bodies. The database
272 attempts to preserve this information through metadata fields describing sampling date, sampling
273 context, and environmental conditions whenever such information was available in the source
274 publications.

275

276 **3.4. Variability related to spatial heterogeneity**

277 Spatial heterogeneity represents another source of uncertainty in the interpretation of isotope
278 patterns. Glacierized catchments often exhibit strong elevation gradients, complex topography,
279 and localized microclimatic conditions that influence precipitation isotope composition and
280 meltwater generation. Isotopic lapse rates associated with altitude can lead to systematic
281 depletion of heavy isotopes at higher elevations, while local factors such as wind redistribution of
282 snow, sublimation, and differential melting may introduce additional variability. Because many
283 compiled studies sampled different parts of a catchment system—such as glacier surfaces,
284 proglacial streams, downstream rivers, or nearby groundwater systems—observed isotope
285 differences may reflect spatial sampling differences rather than inconsistencies in analytical
286 results. Another limitation relates to potential biases in the spatial distribution of available data.
287 Stable isotope measurements in glacierized environments are unevenly distributed
288 geographically, reflecting differences in research infrastructure, accessibility of field sites, and
289 historical research priorities. Well-studied regions such as the European Alps, North American
290 mountain ranges, and parts of Asia tend to have higher densities of isotope measurements
291 compared to remote or logistically challenging glacier regions. As a result, the dataset may not
292 fully capture the global diversity of isotope signatures across all glacierized basins. Users
293 performing global-scale analyses should therefore consider potential regional sampling biases
294 when interpreting spatial patterns or deriving global relationships. For this reason, the geographic
295 coordinates and elevation of sampling locations were retained as core metadata fields to enable



296 spatially explicit analyses and allow users to evaluate potential altitude or catchment-scale
297 effects.

298

299 **3.5. Variability related to metadata**

300 The integration of heterogeneous datasets into a unified database also introduces uncertainty
301 related to data harmonization. Source publications vary in how isotope values are reported,
302 including differences in units, reference scales, coordinate systems, and terminology used to
303 describe sample types. Data were reported to VSMOW-SLAP, 2 point normalization (‰). Records
304 lacking essential contextual information such as geographic location, sample type, or isotope
305 units, were excluded or flagged during quality control procedures. Nevertheless, some degree of
306 uncertainty remains inherent when combining datasets generated under different scientific
307 objectives and reporting frameworks. Metadata completeness represents an additional limitation
308 of the dataset. While the database includes a standardized set of metadata fields describing
309 geographic, environmental, and analytical attributes of each sample, not all publications reported
310 the full set of information. For example, analytical uncertainty values, sampling depth, or detailed
311 descriptions of sampling context were sometimes absent from the original sources. In such cases,
312 the dataset preserves the available information without attempting to infer missing parameters.
313 This approach prioritizes transparency and avoids introducing assumptions that could bias
314 subsequent analyses. However, users should be aware that incomplete metadata may limit
315 certain types of quantitative assessments, particularly those requiring precise information on
316 sampling conditions or laboratory analytical performance. Despite these limitations, the
317 compilation provides several mechanisms that allow users to evaluate and propagate uncertainty
318 in downstream analyses. The standardized classification of endmember types (e.g., precipitation,
319 snowpack, glacier ice, meltwater, groundwater) enables statistical comparison of isotope
320 distributions within and between hydrological components. Measures such as variance,
321 interquartile range, and confidence intervals can be used to quantify the dispersion of isotope
322 values within each category, providing insight into both environmental variability and potential
323 analytical uncertainty. Similarly, regression analyses used to derive global or regional isotope
324 relationships can incorporate statistical measures of uncertainty such as confidence intervals.
325 In summary, uncertainty in this dataset should be interpreted as the combined outcome of
326 analytical precision, environmental variability, methodological differences among studies, and
327 limitations associated with data integration and metadata completeness. The database addresses



328 these challenges through transparent documentation, metadata standardization, and quality-
329 control procedures designed to maximize comparability among records while preserving the
330 contextual information necessary for scientific interpretation. Users are encouraged to consider
331 these sources of uncertainty when applying the dataset to hydrological analyses, isotope-based
332 mixing models, or regional comparisons of water isotope signatures in glacierized catchments.

333

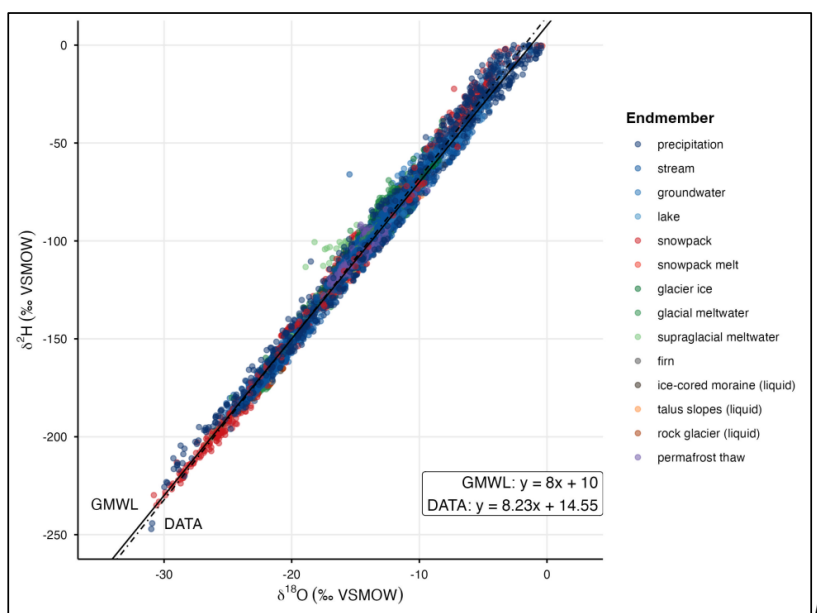
334 **4. Results and discussions**

335 **4.1. Distribution of cryosphere and hydrological endmembers**

336 Data were plotted using a Dual-isotope diagram ($\delta^2\text{H}$ vs. $\delta^{18}\text{O}$, ‰ VSMOW) showing the
337 distribution of cryosphere and hydrological endmembers compiled from glacierized catchments
338 (Figure 2). Most observations cluster along the GMWL (GMWL: $\delta^2\text{H} = 8 \cdot \delta^{18}\text{O} + 10$; Craig, 1961),
339 the isotope signatures therefore largely preserve the original meteoric signal. The possible
340 dominant influence of high-altitude and cold climate in glacierized catchments can result in
341 minimal kinetic fractionation and endmembers isotopic compositions that remain close to the
342 GMWL (Gibson et al., 2002). All waters display negative $\delta^2\text{H}$ values relative to VSMOW and
343 VSMOW2, reflecting precipitation formed under progressive rainout during atmospheric
344 transport and inherited by glacier, firn, meltwater, groundwater, and lake components with
345 limited post-depositional fractionation and preservation of the original climatic signal (Olliver et
346 al., 2025). The general regression line shows a slope close to that of the global meteoric water
347 (8.23), indicating isotope fractionation dominated by equilibrium condensation rather than
348 evaporation. The relatively high intercepts ($\approx 15\text{‰}$) correspond to elevated d-excess values and
349 reflect evaporation under non-equilibrium conditions at the moisture source (e.g., in atmospheres
350 with low relative humidity, Pfahl and Sodemann, 2014). Precipitation in cold and high-latitude
351 regions often originates from cold oceans, sea-ice margins, or continental surfaces where the air
352 is dry. These characteristics are commonly associated with cold-season precipitation and long-
353 range atmospheric transport, and they are preserved in snow, ice, meltwater, and downstream
354 waters due to minimal post-precipitation evaporation (Merlivat and Jouzel, 1979). Liquid waters
355 derived from cryosphere environments (ice-cored moraine, talus slopes, supraglacial meltwater,
356 rock glacier outflow, and permafrost thaw) also plot close to the GMWL. Stream and lake waters
357 show comparable patterns, overlapping with precipitation, snowpack, and glacial meltwater. This
358 implies that precipitation, snowmelt, and glacial melt entering the system at different times are
359 mixed and averaged through storage and transport processes. As a result, short-term or seasonal



360 isotopic variability is not observed. For the lake endmember, this behaviour particularly contrasts
361 with observations from arid and semi-arid regions, where lakes often show pronounced
362 enrichment in heavier isotopes and deviation from the meteoric water line due to high
363 evaporation, long residence times, and warm climatic conditions and therefore plot along the
364 Global Evaporation Line for Lakes, GEL: $\delta^2\text{H} = 5.5 \cdot \delta^{18}\text{O} - 3$ (e.g., Vystavna et al., 2021).
365



366
367 *Figure 2. Dual-isotope diagram ($\delta^2\text{H}$ vs. $\delta^{18}\text{O}$, ‰ VSMOW) showing the distribution of cryosphere*
368 *and hydrological endmembers compiled from glacierized catchments worldwide. Coloured*
369 *symbols represent different water types, including precipitation, stream, lakes, groundwater,*
370 *snowpack, snowpack melt, glacial meltwater, supraglacial meltwater, firn, glacier ice, ice-core*
371 *moraines, rock glacier, permafrost thaw, and talus slopes. The Global Meteoric Water Line*
372 *(GMWL: $\delta^2\text{H} = 8 \cdot \delta^{18}\text{O} + 10$) is shown for reference.*

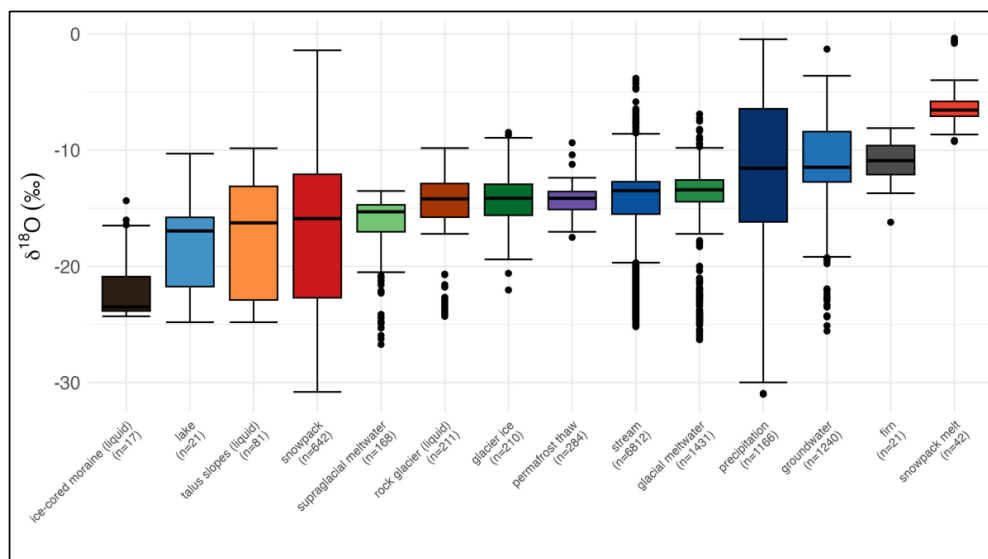
373

374 **4.2. Global variations of stable water isotopes values in hydrological and cryosphere** 375 **endmembers**

376 The boxplots in Figure 3 summarize $\delta^{18}\text{O}$ (‰ VSMOW and VSMOW2) across the compiled global
377 dataset, grouped by hydrological endmember types. Ice-cored moraines, lake, talus-slopes,
378 snowpack and supraglacial meltwater, exhibit the most ^{18}O -depleted isotopic signatures,



379 generally, between -25 and -10‰ . These values are consistent with derivation from long-term
380 snow and ice accumulation formed under cold conditions and limited post-depositional
381 modification (Taylor et al., 2001; Penna et al., 2014) during repeated melt and freeze cycles. Unlike
382 lowland (Aichner et al., 2022) or arid settings, the lakes in this dataset do not show strong isotopic
383 enrichment. Their median value of $\delta^{18}\text{O}$ of approximately -17‰ overlap with those of other cold-
384 region surface waters. This pattern is consistent with the dominance of high-altitude, cold
385 environments, where ice-free periods are short and evaporation is limited (Gat, 1996; Gibson &
386 Edwards, 2002). Isotopic signatures of surface water endmembers, lakes and streams, are
387 consistent with the values in the region established by Li et al. (2025b). Glacier ice, rock glacier,
388 permafrost thaw, stream and glacial meltwater exhibit slightly less ^{18}O -depleted isotopic
389 signatures (approximately -15‰). Snowpack and glacial meltwater display a broad variability
390 possibly due to the diversity of sampling methods and melting approach before analysis that are
391 not standardized yet. Sampling cryosphere endmembers is still a challenge. Also, seasonal snow
392 reflects the precipitation variability. Seasonal fractionation during snowfall, redistribution within
393 the snowpack, and progressive enrichment in heavy isotopes during melt and refreezing cycles
394 (Dansgaard, 1964; Jouzel and Souchez, 1982; Taylor et al., 2001) can also explain the high
395 variability in snowpacks. This comparison may benefit from clearer spatial and temporal
396 constraints (e.g., elevation, season). for instance, in monsoon-dominated regions such as Yulong
397 Snow Mountain, Lijiang, snowpack meltwater has been observed to be isotopically heavier than
398 rainwater (Pu et al., 2020; Shi et al., 2020). Precipitation exhibits the widest spread of $\delta^{18}\text{O}$ values,
399 extending from -30 to 0‰ , capturing the combined effects of latitude, elevation, temperature,
400 and moisture source variability.



401

402 *Figure 3. Boxplots showing the distribution of $\delta^{18}\text{O}$ (‰) values across cryosphere and*
403 *hydrological endmembers in glacierized catchments. Each box represents the median,*
404 *interquartile range, and variability of isotopic composition for a given water type, with*
405 *whiskers indicating data spread and points representing outliers. Sample sizes (n) are*
406 *indicated for each category along the x-axis. The figure illustrates systematic isotopic*
407 *differences among solid cryosphere components (firm, snowpack, glacier ice), liquid*
408 *meltwater sources, groundwater, and precipitation, highlighting enrichment trends*
409 *associated with melt processes, evaporation, and hydrological mixing.*

410

411 **4.3. Continental variations of stable water isotopes values in hydrological and** 412 **cryosphere endmembers**

413 The boxplots in Figure 4 illustrate continental-scale variations in $\delta^{18}\text{O}$ for selected hydrological
414 endmembers across Africa, Asia, Europe, North America, and South America. To represent major
415 climatic and hydrological contrasts across North America, the boxplots were separated at 60°
416 latitude, which marks the transition between sub-Arctic/Arctic and temperate–alpine
417 environments. Regions north of 60°, including Alaska, Yukon, and the Canadian Arctic Archipelago,
418 are characterized by persistently cold conditions, widespread permafrost, and precipitation
419 dominated by cold-season snowfall formed under low temperatures and long atmospheric
420 transport pathways (Pfahl & Sodemann, 2014; Terzer-Wassmuth et al., 2021; Chen et al., 2020).



421 These conditions lead to strong isotopic fractionation and very low $\delta^{18}\text{O}$ and $\delta^2\text{H}$ values, with d-
422 excess primarily reflecting moisture-source characteristics (Dansgaard, 1964). In contrast, regions
423 south of 60° are dominated by temperate and alpine climates with longer melt seasons, more
424 diverse precipitation regimes, and a stronger influence of local moisture recycling and secondary
425 evaporation.

426 These climatic differences are directly reflected in the isotopic composition of hydrological
427 endmembers. North of 60° , glacier ice, meltwater, snowpack, groundwater, and streams exhibit
428 very low $\delta^{18}\text{O}$ values, with median values frequently below -20‰ , indicative of cold continental
429 and high-latitude environments. Stream waters reflect mixing between cryosphere and meteoric
430 sources, resulting in intermediate values that nonetheless indicate a dominant contribution from
431 glacier and snowmelt. South of 60° , all endmembers shift towards less negative isotope values.
432 Although glacier ice and meltwater remain relatively ^{18}O -depleted, precipitation and groundwater
433 are more ^{18}O -enriched (typically around -15 to -10‰), consistent with milder conditions and
434 greater influence of lower-latitude moisture sources, while streams display a broad range of
435 values reflecting variable source mixing (Zang et al., 2024). Overall, North America exhibits the
436 widest range of isotope values among the continents considered in this study, reflecting strong
437 latitudinal and elevational gradients combined with contrasting precipitation regimes and
438 complex hydrological mixing processes (Dansgaard, 1964; Bowen and Revenaugh, 2003). Similar
439 numbers of isotope measurements are available for both North America and Asia, and more for
440 Europe, suggesting the greater variability observed in North America is real rather than a sample
441 size artefact.

442 South America exhibits marked isotopic gradients influenced by the Andean uplift and the
443 contribution of moisture sources from the Amazon and the Pacific. In high mountain areas, such
444 as Nevado Huascarán (Cordillera Blanca, Peru), glacial meltwater shows depleted $\delta^{18}\text{O}$ values
445 (typically between -18 and -14‰), resulting from orographic uplift and the progressive depletion
446 of heavy isotopes from the Amazonian source (Insel, 2013; Apaéstegui et al., 2023; Vargas et al.,
447 2022). However, analysis of ice cores extracted in 2019 reveals that, while the isotopic record
448 ($\delta^{18}\text{O}$) at a regional scale responds to the climatic variability of the tropical Pacific (especially in
449 the NINO3.4 region) and to El Niño-related teleconnections that modulate precipitation over the
450 Amazon basin, at a local scale its variability is more determined by changes in atmospheric
451 temperature than by precipitation itself. This distinction explains why, in contrast to the regional
452 signal, precipitation and groundwater in lower-lying areas show greater variability and isotopic



453 enrichment, suggesting a more direct influence of warmer temperatures (Vuille et al., 2003). Over
454 the past 60 years, the relationship between climate and $\delta^{18}\text{O}$ in these glaciological archives has
455 intensified in parallel with atmospheric and oceanic warming, as well as modifications in the
456 Walker circulation, demonstrating its sensitivity to recent climate change.

457 In Africa, data coverage is limited and largely restricted to liquid waters. Precipitation, streams,
458 and groundwater show relatively high $\delta^{18}\text{O}$ values, with medians generally between -10‰ and
459 -7‰ . Africa is characterized by generally higher $\delta^{18}\text{O}$ and $\delta^2\text{H}$ values compared to high-latitude
460 regions, reflecting warmer temperatures and dominant convective rainfall regimes. Because
461 equilibrium fractionation decreases at higher temperatures, precipitation tends to be less
462 depleted in heavy isotopes, consistent with tropical hydroclimatic conditions (Gat & Matsui, 1991;
463 Rozanski et al., 1996). Moisture supplying high-mountain precipitation in East and Central Africa
464 is primarily derived from the Indian Ocean and regional continental recycling (Levin et al., 2009).
465 The limited representation related endmember reflects the scarcity of extensive cryosphere
466 environments across the continent and highlights the need for expanded isotopic sampling in
467 African mountain regions to better constrain hydrological responses to climate change.

468 Asia exhibits a broad isotopic range driven by strong topographic and climatic gradients.
469 Snowpack and glacier ice are particularly depleted in heavy isotopes, with median $\delta^{18}\text{O}$ values
470 typically between -15 and -12‰ , showing high-elevation snowfall and intense Rayleigh
471 distillation over the Himalaya–Tibetan Plateau (Yao et al., 2013). Higher, colder mountains (like
472 the Himalaya–Tibetan Plateau) induce stronger Rayleigh distillation, resulting in more negative
473 $\delta^{18}\text{O}$ values. Glacial meltwater retains similarly low SWI values but with greater spread, while
474 streams and groundwater cluster around -12 to -9‰ , consistent with mixing between ^{18}O -
475 depleted cryosphere sources and relatively ^{18}O -enriched monsoon precipitation (Immerzeel et al.,
476 2010). In some cases, the variability might arise from mixing with precipitation or snowmelt, or
477 from the selection of sampling sites, rather than intrinsic fluctuations in the glacier meltwater
478 itself. The pronounced variability in $\delta^{18}\text{O}$ values across endmembers is indicative of the region's
479 complex interplay between elevation, atmospheric circulation, and moisture sources. This
480 diversity is further illustrated by the wide interquartile ranges in the boxplots (Fig. 5), which
481 capture both the strong depletion in high-altitude environments and the enrichment associated
482 with lowland rainfall and groundwater recharge.

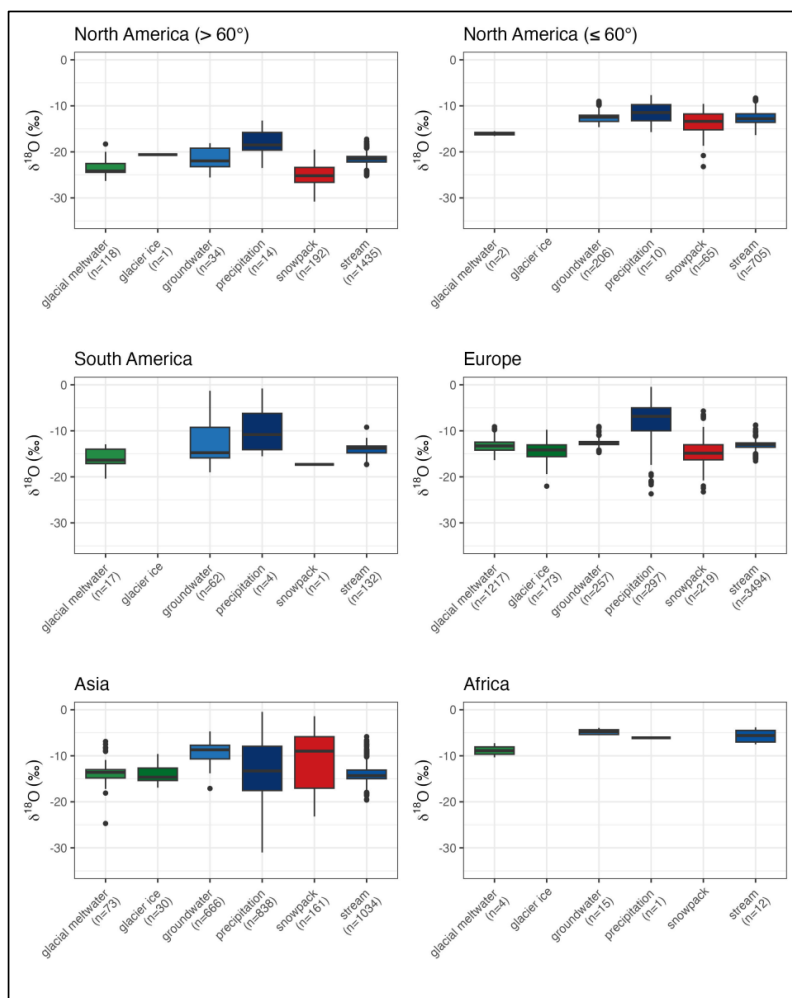
483 European waters show moderate ^{18}O -depletion and comparatively narrow interquartile ranges.
484 This is probably due to this very limited area of investigations (latitude limited data) with no data



485 from northern EU. Glacier ice, streams, and groundwater typically fall between -12 and -8% ,
486 reflecting mid-latitude precipitation regimes, westerly moisture transport, and a weaker altitude
487 effect relative to high mountain regions (Rozanski et al., 1993; Stumpp et al., 2014). The reduced
488 variability in streams and groundwater highlights buffering and seasonal averaging, perhaps
489 stronger than other continents, which lower isotopic extremes and produce more stable
490 signatures over time. The relatively limited spread in $\delta^{18}\text{O}$ values across endmembers in this part
491 of Europe, as shown in Figure 5, suggests that regional hydrology is dominated by moderate
492 climatic gradients and efficient mixing of water sources, in contrast to the more pronounced
493 variability observed in Asia, North America and South America.

494 In Oceania, the available data are extremely limited, with only a single endmember represented
495 in the dataset. As a result, it is not possible to draw meaningful conclusions or interpret regional
496 isotopic patterns for this continent.

497 These continental patterns suggest the dominant controls on water isotope variability with
498 following evident: temperature and altitude effects driving heavy isotope depletion in cold and
499 high-elevation regions, atmospheric circulation shaping regional gradients, evaporation enriching
500 surface and near-surface waters with heavy isotopes in warm climates, and hydrological mixing
501 buffering isotopic extremes in streams and groundwater (Dansgaard, 1964; Rozanski et al., 1993;
502 Gat, 1996; Kendall & McDonnell, 1998; Gibson & Edwards, 2002).



503

504 *Figure 4. Continental-scale variability in $\delta^{18}\text{O}$ (‰) for major hydrological and cryosphere*
505 *endmembers across glacierized regions. Boxplots show regional distributions for North America*
506 *(>60° and ≤60° latitude), South America, Europe, Asia, and Africa, illustrating differences in*
507 *isotopic depletion related to latitude, elevation, and climatic setting. Sample sizes (n) are indicated*
508 *for each endmember.*

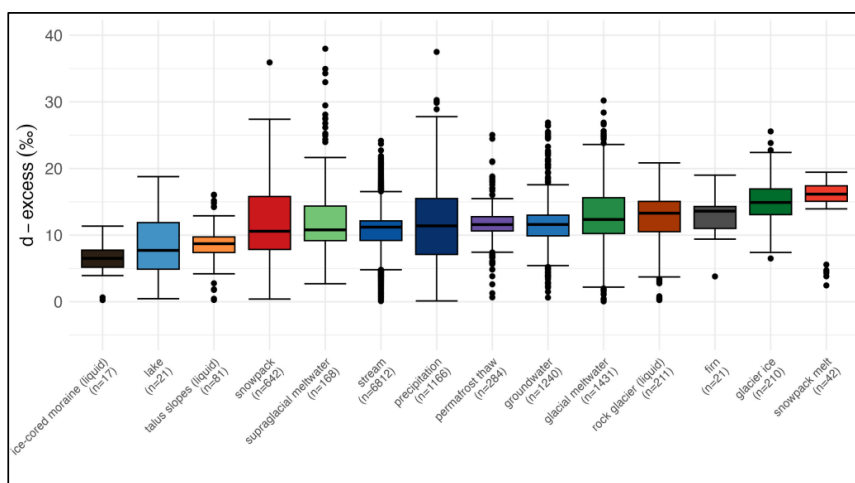
509

510 **4.4. Deuterium excess and moisture source in hydrological and cryosphere endmembers**

511 The d-excess distributions shown in Figure 5 show the moisture source conditions. Overall, most
512 endmembers cluster around positive d-excess values (roughly 8–15‰), indicating that the
513 primary precipitation isotopic signal is preserved across the dataset and that moisture sources



514 were largely characterized by non-equilibrium conditions at the ocean–atmosphere interface.
515 Low relative humidity, strong wind speeds, or cooler sea surface temperatures enhance kinetic
516 fractionation during evaporation, increasing d-excess in the resulting vapor and, ultimately, in
517 precipitation. Snowpack and glacier ice display the highest median d-excess values (typically ~14–
518 18‰), consistent with cold-season precipitation and high-elevation snowfall, where kinetic
519 fractionation during vapor formation and condensation enhances d-excess (Dansgaard, 1964;
520 Pfahl & Sodemann, 2014). Cryosphere-derived meltwaters (supraglacial meltwater, glacial
521 meltwater) show slightly lower and more variable d-excess. This suggests post-depositional
522 modification during sublimation, melting, refreezing, and surface exposure, where partial
523 evaporation and exchange with atmospheric moisture tend to reduce d-excess. Streams and
524 groundwater occupy intermediate ranges, typically have d-excess of 10–12‰, consistent with the
525 mixing of multiple sources and hydrological buffering that smooths variabilities (Kendall &
526 McDonnell, 1998; Jasechko et al., 2014). Lakes, talus-slope, and ice-cored moraine waters exhibit
527 lower median d-excess values and broader spreads, in some cases approaching or dropping below
528 ~8‰. This pattern is indicative of evaporation under sub-saturated conditions. The relatively wide
529 interquartile ranges in these open waters suggest variable residence times and differing degrees
530 of evaporation (Gat, 1996; Gibson et al., 2008). Permafrost thaw waters show moderate d-excess
531 values but with substantial scatter, highlighting their transitional nature between stored
532 cryosphere ice and active hydrological endmember. Variability likely reflects heterogeneity in ice
533 age, freezing history, and subsequent interaction with soil water during thaw (Yang et al., 2024).
534



535



536 *Figure 5: Global distribution of d-excess (‰) across cryosphere and hydrological endmembers.*
537 *Boxplots illustrate variability in d-excess values among liquid and solid water sources, including*
538 *precipitation, stream, lakes, groundwater, snowpack, snowpack melt, glacial meltwater,*
539 *supraglacial meltwater, firn, glacier ice, ice-core moraines, rock glacier, permafrost thaw, and*
540 *talus slopes. Median values, interquartile ranges, and outliers highlight differences in moisture*
541 *source conditions, evaporative processes, and secondary fractionation effects influencing isotopic*
542 *signatures across glacierized catchments worldwide.*

543

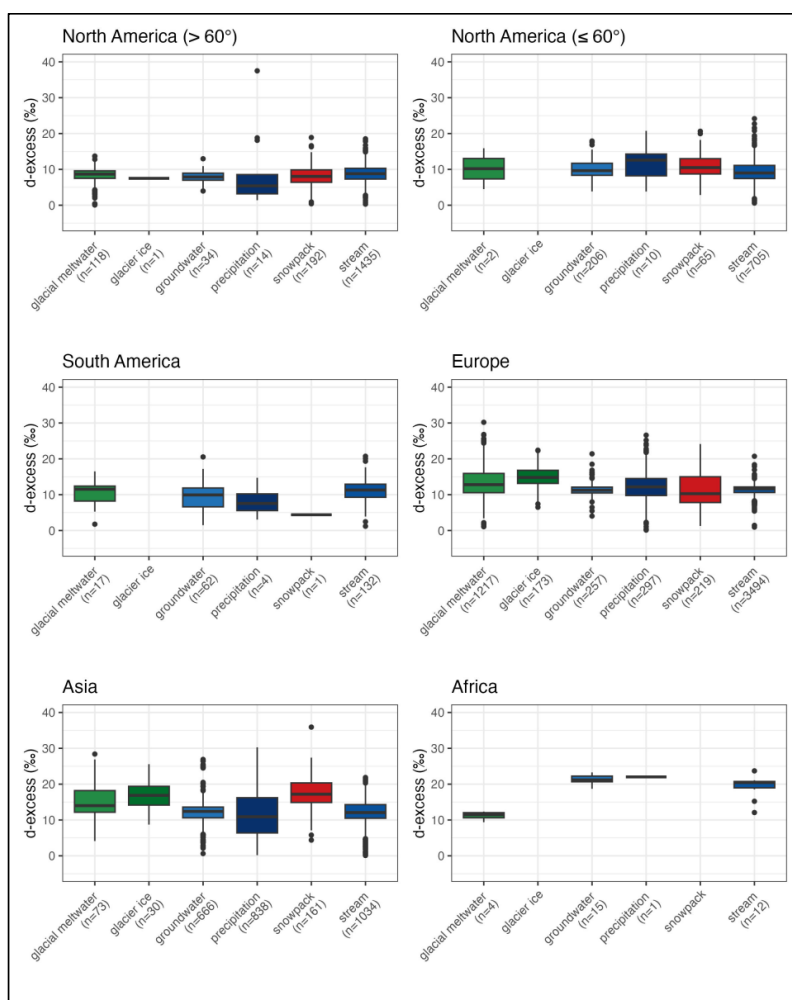
544 Figure 6 shows clear intercontinental differences in d-excess, reflecting variations in moisture
545 source conditions, atmospheric transport pathways, precipitation seasonality, and post-
546 depositional modification. Because d-excess is primarily established during oceanic evaporation,
547 relative humidity and sea-surface temperature at the moisture source exert first-order control.
548 Low relative humidity and strong kinetic fractionation at the interface generate higher d-excess,
549 whereas evaporation under humid conditions produces lower values.

550 This is evident in Asia, where elevated median d-excess (>10‰) reflects a strong influence of
551 moisture derived from relatively dry, cool oceanic sources. In parts of Central and Inner Asia, long
552 transport pathways and cold-season snowfall further contribute to elevated d-excess in
553 cryosphere components. Snowpack and glacier ice frequently preserve winter precipitation
554 signals formed under lower humidity conditions, resulting in higher median values relative to
555 groundwater and streams. In contrast, South America and lower-latitude regions of North
556 America show lower median d-excess and broader distributions, consistent with a greater
557 contribution from warm and humid tropical moisture sources and enhanced continental recycling
558 during atmospheric transport (Chen et al., 2020; Kim et al., 2025). Continental recycling and sub-
559 cloud evaporation reduces d-excess (Pfahl & Sodemann, 2014). In regions with long atmospheric
560 transport pathways and strong continental recycling (e.g., parts of Asia and South America),
561 precipitation can experience evaporation during descent or mixing with recycled moisture,
562 increasing scatter and often lowering d-excess (Pfahl & Sodemann, 2014; Terzer-Wassmuth et al.,
563 2021). At higher latitudes (>60°N), North America shows moderately elevated values,
564 nevertheless, values remain lower than in some Asian regions, likely reflecting dominant Pacific
565 moisture influence.

566 Europe shows intermediate to moderately high median d-excess values across most hydrological
567 components, with relatively broad distributions, particularly in precipitation and glacier



568 meltwater. This pattern reflects the superposition of multiple moisture sources and strong
569 seasonal contrasts. Africa exhibits comparatively high median d-excess, particularly in
570 groundwater and precipitation. This pattern is consistent with moisture derived from relatively
571 dry source regions under low humidity. Under such conditions, kinetic effects during vapor
572 formation enhance d-excess. However, the African dataset is limited in size and cryosphere
573 representation, and precipitation and stream categories are sparsely sampled. The narrow
574 distribution therefore likely reflects the scarcity of the dataset structure rather than a
575 homogeneous continental signal. The elevated values should be interpreted cautiously.
576



577

578 *Figure 6: Continental-scale variability in d-excess (‰) across major cryosphere and hydrological*



579 *endmembers. Boxplots illustrate regional distributions for North America (>60° and ≤60° latitude),*
580 *South America, Europe, Asia, and Africa, highlighting differences in moisture source conditions,*
581 *evaporation effects, and atmospheric processes influencing isotopic signatures. Variability among*
582 *precipitation, snowpack, glacier-derived waters, groundwater, and streams reflect regional*
583 *climatic gradients and mixing processes, with sample sizes (n) indicated for each endmember.*

584

585 **4.6. Implications for Isotope Hydrology in Glacierized catchments**

586 Global and continental-scale pairwise statistical comparisons of $\delta^{18}\text{O}$ among major cryosphere and
587 hydrological endmembers reveal clear differences in isotopic separation strength on the global
588 scale and between regions, largely controlled by climatic gradients, moisture sources, and data
589 availability (Figures S1 and S2 in supplementary Information). The post-hoc Dunn's test results
590 indicate that most cryosphere and hydrological endmembers are statistically distinguishable
591 based on their stable isotope compositions ($p < 0.05$), demonstrating a generally robust
592 separation among major water sources. Precipitation exhibits statistically significant SWI
593 differences ($p < 0.05$) from most other endmembers, including glacier ice, meltwaters,
594 groundwater, lake, stream, indicating that its primary atmospheric signal is substantially modified
595 during storage and transport within the catchment. In contrast, liquid endmembers display
596 greater internal similarity and more frequent non-significant differences, consistent with rapid
597 mixing and short residence times. Multiple cycles of melting and refreezing mean that the
598 snowpack endmember varies to the point it is not significantly different from all other
599 endmembers when considering the global dataset. Waters derived from rock glaciers, ice-cored
600 moraines, and talus slopes remain significantly distinct, suggesting additional fractionation and
601 storage effects.

602 Europe shows the strongest and most systematic statistical separation between endmembers.
603 Most pairwise comparisons are highly significant ($p < 0.001$), indicating well-defined isotopic
604 distinctions between precipitation, snowpack, glacial meltwater, groundwater, and streams. This
605 likely reflects strong seasonal contrasts, elevation gradients in the Alps, and relatively dense
606 datasets. Asia also exhibits widespread significant differences, although slightly less uniform than
607 Europe. Strong contrasts between snowpack, precipitation, and groundwater suggest
608 pronounced variability in moisture origin and secondary fractionation across High Mountain Asia.
609 The influence of monsoonal inputs and continental recycling probably enhances d-excess
610 variability, increasing separability among endmembers. North America (>60°) shows moderate



611 differentiation. Significant contrasts mainly occur between glacial meltwater, precipitation, and
612 stream water, whereas glacier ice itself appears less distinct, possibly reflecting overlapping
613 moisture source conditions or limited sample numbers. In contrast, North America ($\leq 60^\circ$) shows
614 relatively few significant comparisons, implying greater mixing or weaker climatic gradients at
615 mid-latitudes. South America presents limited statistical separation overall. Only a few
616 comparisons involving stream water and glacial meltwater reach significance, which likely reflects
617 smaller sample sizes and narrower $\delta^{18}\text{O}$ variability within Andean datasets. Similarly, Africa shows
618 minimal significant contrasts; most cells are non-significant or unavailable, consistent with sparse
619 cryosphere representation and limited sampling.

620 Overall, the analysis indicates that $\delta^{18}\text{O}$ is a powerful discriminator of hydrological endmembers
621 in regions with strong atmospheric gradients and robust datasets (Europe, Asia), whereas in
622 regions with limited cryosphere presence or smaller sample sizes (Africa, parts of South America),
623 statistical differentiation remains weak. The important variability observed within endmembers
624 such as snowpack, meltwaters, precipitation, and streams highlights the strong influence of local
625 conditions and the timing of sampling. Also, precipitation is mostly sampled on a monthly time
626 scale, but the variability of daily samples can be even greater (Saidaliyeva et al., 2024) while other
627 components are mostly result of snapshot sampling campaigns. This variability makes clear that
628 endmembers need to be defined with care (only use in analysis those endmembers that have a
629 clear, significant separation from other) and that uncertainty should be explicitly considered when
630 using isotopes for mixing analyses or hydrograph separation (Christophersen & Hooper, 1992;
631 Barthold et al., 2011, Popp et al., 2025).

632

633 **5. Conclusions and Applications**

634

635 The preparation of the database (Vital et al., 2026) revealed several recurring gaps in how isotope
636 data is reported, which reduce their usability for comparative analyses and modelling
637 applications. In many studies, sampling locations are not described with sufficient spatial
638 precision, with coordinates missing, rounded, or limited to general catchment descriptions.
639 Information on analytical procedures is often incomplete, including the type of instrument used,
640 calibration protocols, or reference standards, and analytical uncertainties are not always provided
641 in a consistent way. Another common limitation is the reporting of isotope results only as
642 averages or ranges, without access to individual sample values and sampling dates, which restricts



643 the evaluation of temporal variability and uncertainty. Highlighting these issues and encouraging
644 more complete metadata reporting would improve data transparency and facilitate the
645 integration of future datasets into regional and global isotope compilations.

646 The studied spatial distribution of stable water isotopes in glacierized catchments provides a
647 framework for interpreting endmember contributions and supports the application of isotope-
648 based mixing approaches in glacierized and non-glacierized catchments worldwide. The dataset
649 can be used as a baseline for multiple applications in hydrology, climate science, and water
650 management. Particularly, isotope data can be applied in endmember mixing analysis to partition
651 the streamflow into contributions from snowmelt, glacier melt, and groundwater. This is
652 especially relevant in mountain catchments where seasonal water supply depends on cryosphere
653 sources (Kendall & McDonnell, 1998). Additionally, ice cores preserve isotope signatures of past
654 precipitation. By linking modern endmember isotopes with paleoclimate records, this dataset can
655 support the reconstruction of past hydrological regimes and climate change (Rozanski et al.,
656 1992). Finally, this dataset provides benchmarks for isotope-enabled hydrological models (e.g.,
657 iCESM, IsoHydro, JAMS200). The interpretations, presented here, of this unique global dataset are
658 a beginning, and we believe that making these data available to the community will help facilitate
659 more in-depth investigation of the key factors and processes determining the hydrology of
660 glacierized catchments measured through water stable isotope ratios. Understanding temporal
661 and spatial variations in the stable isotopic composition of cryosphere and hydrological
662 components is essential and crucial for sustainable water resource management because of
663 climate change, land use changes and human activities impact aquifer recharge, as well as surface
664 and groundwater quality and quantity (Gačnik et al, 2026). Therefore, it is crucial to perform long-
665 term isotope monitoring, continue with updating the database, to ensure the traceability of water
666 isotope data, to provide results comparable in space and time, and to implement the FAIR data
667 practice into daily research, following the goals of the Global Analysis laboratory Network
668 (GloWAL) - IAEA.

669

670 **Data availability**

671 Data described in this manuscript can are publicly available through the ZENODO data repository.
672 The dataset can be accessed at: <https://doi.org/10.5281/zenodo.19062383>.

673

674 **Software**



675 The codes used in this study are available publicly available through the ZENODO data repository.

676 The codes can be accessed at: <https://doi.org/10.5281/zenodo.18982251>

677

678 **Author contributions**

679 Conceptualization (MV, YV, AW, JMD, AP, PV), data curation: (All authors), formal analysis (MV,
680 EJ, YV, AW, JMD, AP), funding acquisition (YV, MV), methodology (MV, YV), software (EJ),
681 supervision (MV, YV), validation: (MV, YV, AW, JMD, AP, PV), visualization (EJ, MV), writing –
682 original draft preparation (MV, YV, AW, JMD, AP, MT, PV), writing – review and editing: All
683 authors.

684

685 **Competing interests**

686 The authors declare that they have no conflict of interest.

687

688 **Acknowledgements**

689 The authors gratefully acknowledge all researchers, institutions, and national partners who
690 contributed data and technical input to the development of the database, as well as colleagues
691 who provided scientific feedback during its compilation and quality control. Special thanks are
692 extended to Ms Sarah Sapper (Formerly IAEA intern) for her dedicated support in compiling,
693 organizing, and harmonizing the datasets.

694

695 **Financial support**

696 Coordinated Research project F33031 “Understanding Hydrological Processes in Glacierized
697 catchments under Changing Climate using Isotope Techniques” from the International Atomic
698 Energy Agency.

699

700 **References**

701 Aichner, B., Dubbert, D., Kiel, C., Kohnert, K., Ogashawara, I., Jechow, A., Harpenslager, S.-F.,
702 Hölker, F., Nejtgaard, J. C., Grossart, H.-P., Singer, G., Wollrab, S., and Berger, S. A.: Spatial
703 and seasonal patterns of water isotopes in northeastern German lakes, Earth Syst. Sci.
704 Data, 14, 1857–1867, <https://doi.org/10.5194/essd-14-1857-2022>, 2022.

705 Ala-Aho, P., Tetzlaff, D., McNamara, J. P., Laudon, H., and Soulsby, C.: Using isotopes to constrain
706 water flux and age estimates in snow-influenced catchments using the STARR (Spatially
707 distributed Tracer-Aided Rainfall–Runoff) model, Hydrol. Earth Syst. Sci., 21, 5089–5110,
708 <https://doi.org/10.5194/hess-21-5089-2017>, 2017.

709 Amschwand, D., Tschan, S., Scherler, M., Hoelzle, M., Krummenacher, B., Haberkorn, A., and



- 710 Gubler, H.: Seasonal ice storage changes and meltwater generation at Murtèl rock glacier
711 (Engadine, eastern Swiss Alps): estimates from measurements and energy budgets in the
712 coarse blocky active layer, *Hydrol. Earth Syst. Sci.*, 29, 2219–2253,
713 <https://doi.org/10.5194/hess-29-2219-2025>, 2025.
- 714 Apaéstegui, J., Romero, C., Vuille, M., Sulca, J., and Ampuero, A.: Moisture sources and rainfall
715 $\delta^{18}\text{O}$ variability over the Central Andes of Peru—A case study from the Mantaro River
716 Basin, *Water*, 15, 1867, <https://doi.org/10.3390/w15101867>, 2023.
- 717 Avesani, D., Nan, Y., and Tian, F.: Reducing hydrological uncertainty in large mountainous basins:
718 the role of isotope, snow cover, and glacier dynamics in capturing streamflow seasonality,
719 *Hydrol. Earth Syst. Sci.*, 29, 5755–5775, <https://doi.org/10.5194/hess-29-5755-2025>,
720 2025.
- 721 Bai, H., Rupper, S., and Strong, C.: Brief communication: Impact of mountain glaciers on regional
722 hydroclimate, *EGUsphere* [preprint], <https://doi.org/10.5194/egusphere-2025-675>,
723 2025.
- 724 Barthold, F. K., Tyralla, C., Schneider, K., Vaché, K. B., Frede, H.-G., and Breuer, L.: How many
725 tracers do we need for end member mixing analysis (EMMA)?, *Water Resour. Res.*, 47,
726 W08519, <https://doi.org/10.1029/2011WR010604>, 2011.
- 727 Bowen, G. J., Cai, Z., Fiorella, R. P., and Putman, A. L.: Isotopes in the water cycle: regional- to
728 global-scale patterns and applications, *Annu. Rev. Earth Planet. Sci.*, 47, 453–479,
729 <https://doi.org/10.1146/annurev-earth-053018-060220>, 2019.
- 730 Bowen, G. J., and Revenaugh, J.: Interpolating the isotopic composition of modern meteoric
731 precipitation, *Water Resour. Res.*, 39, 1299, <https://doi.org/10.1029/2003WR002086>,
732 2003.
- 733 Chen, L., Wang, Q., Zhu, G., Lin, X., Qiu, D., Jiao, Y., Lu, S., Li, R., Meng, G., and Wang, Y.: Dataset
734 of stable isotopes of precipitation in the Eurasian continent, *Earth Syst. Sci. Data*, 16,
735 1543–1557, <https://doi.org/10.5194/essd-16-1543-2024>, 2024.
- 736 Chen, Y., Yang, H., Li, C., and Liu, Z.: Quantifying the warming-induced impact of glacier storage
737 change on runoff using Budyko framework: a case study in the Tarim River basin, *J. Hydrol.*
738 *Reg. Stud.*, 55, 101936, <https://doi.org/10.1016/j.ejrh.2024.101936>, 2024.
- 739 Christophersen, N., and Hooper, R. P.: Multivariate analysis of stream water chemical data: the
740 use of principal components analysis for the end-member mixing problem, *Water Resour.*
741 *Res.*, 28, 99–107, <https://doi.org/10.1029/91WR02518>, 1992.
- 742 Clark, I. D., and Fritz, P.: *Environmental Isotopes in Hydrogeology*, CRC Press,
743 <https://doi.org/10.1201/9781482242911>, 1997.
- 744 Craig, H.: Isotopic variations in meteoric waters, *Science*, 133, 1702–1703,
745 <https://doi.org/10.1126/science.133.3465.1702>, 1961.
- 746 Curry, A. M.: Talus slopes, Reference Module in Earth Systems and Environmental Sciences,
747 <https://doi.org/10.1016/B978-0-323-99931-1.00047-7>, 2023.
- 748 Dansgaard, W.: Stable isotopes in precipitation, *Tellus*, 16, 436–468,
749 <https://doi.org/10.1111/j.2153-3490.1964.tb00181.x>, 1964.
- 750 Dee, S., Bailey, A., Conroy, J. L., et al.: Water isotopes, climate variability, and the hydrological
751 cycle: recent advances and new frontiers, *Environ. Res. Clim.*, 2, 022002,
752 <https://doi.org/10.1088/2752-5295/acbe1>, 2023.
- 753 Evans, M. N., Lücke, L. J., Fan, K. J., and Zhu, F.: A database of databases for Common Era
754 paleoclimate applications, *Earth Syst. Sci. Data*, 18, 1185–1202,
755 <https://doi.org/10.5194/essd-18-1185-2026>, 2026.
- 756 Fierz, C., Armstrong, R. L., Durand, Y., Etchevers, P., Greene, E., McClung, D. M., Nishimura, K.,
757 Satyawali, P. K., and Sokratov, S. A.: The International Classification for Seasonal Snow on



- 758 the Ground, UNESCO-IHP, Paris, 2009.
- 759 Gat, J. R.: Oxygen and hydrogen isotopes in the hydrologic cycle, *Annu. Rev. Earth Planet. Sci.*, 24,
760 225–262, <https://doi.org/10.1146/annurev.earth.24.1.225>, 1996.
- 761 Gat, J. R., and Matsui, E.: Atmospheric water balance in the Amazon Basin: an isotopic
762 evapotranspiration model, *J. Geophys. Res.*, 96, 13179–13188,
763 <https://doi.org/10.1029/91JD00054>, 1991.
- 764 Gačnik, J., Žagar, K., Hatvani, I. G., Kern, Z., and Vreča, P.: Climate change reflected in 40-year
765 isotopic composition trends of precipitation in Slovenia, *Environ. Res.*,
766 <https://doi.org/10.1016/j.envres.2025.123286>, 2025.
- 767 Gibson, J. J., and Edwards, T. W. D.: Regional water balance trends and evaporation–transpiration
768 partitioning from a stable isotope survey of lakes in northern Canada, *Global Biogeochem.*
769 *Cycles*, 16, 1026, <https://doi.org/10.1029/2001GB001839>, 2002.
- 770 Glas, R., Lautz, L., McKenzie, J., Mark, B., Baraer, M., Chavez, D., and Maharaj, L.: A review of the
771 current state of knowledge of proglacial hydrogeology in the Cordillera Blanca, Peru,
772 *WIREs Water*, 5, e1299, <https://doi.org/10.1002/wat2.1299>, 2018.
- 773 Gordon, R. P., Lautz, L. K., McKenzie, J. M., Mark, B. G., Chávez, D., and Baraer, M.: Sources and
774 pathways of stream generation in tropical proglacial valleys of the Cordillera Blanca, Peru,
775 *J. Hydrol.*, 522, 628–644, <https://doi.org/10.1016/j.jhydrol.2015.01.013>, 2015.
- 776 Hooper, R. P.: Diagnostic tools for mixing models of stream water chemistry, *Water Resour. Res.*,
777 39, 1055, <https://doi.org/10.1029/2002WR001528>, 2003.
- 778 Horita, J., and Wesolowski, D. J.: Liquid–vapor fractionation of oxygen and hydrogen isotopes of
779 water from the freezing to the critical temperature, *Geochim. Cosmochim. Acta*, 58,
780 3425–3437, [https://doi.org/10.1016/0016-7037\(94\)90096-5](https://doi.org/10.1016/0016-7037(94)90096-5), 1994.
- 781 Humlum, O.: The geomorphic significance of rock glaciers: estimates of rock glacier debris
782 volumes and headwall recession rates in West Greenland, *Geomorphology*, 35, 41–67,
783 [https://doi.org/10.1016/S0169-555X\(00\)00022-2](https://doi.org/10.1016/S0169-555X(00)00022-2), 2000.
- 784 Huss, M., and Hock, R.: Global-scale hydrological response to future glacier mass loss, *Nat. Clim.*
785 *Change*, 8, 135–140, <https://doi.org/10.1038/s41558-017-0049-x>, 2018.
- 786 IAEA: Towards Best Practices in Isotope-Enabled Hydrological Modelling Applications, IAEA-
787 TECDOC-2022, IAEA, Vienna, 2023.
- 788 Immerzeel, W. W., van Beek, L. P. H., and Bierkens, M. F. P.: Climate change will affect the Asian
789 water towers, *Science*, 328, 1382–1385, <https://doi.org/10.1126/science.1183188>, 2010.
- 790 Insel, N., Poulsen, C. J., Sturm, C., and Ehlers, T. A.: Climate controls on Andean precipitation $\delta^{18}\text{O}$
791 interannual variability, *J. Geophys. Res. Atmos.*, 118, 9721–9742,
792 <https://doi.org/10.1002/jgrd.50619>, 2013.
- 793 Jansson, P., Hock, R., and Schneider, T.: The concept of glacier storage: a review, *J. Hydrol.*, 282,
794 116–129, [https://doi.org/10.1016/S0022-1694\(03\)00258-0](https://doi.org/10.1016/S0022-1694(03)00258-0), 2003.
- 795 Jasechko, S., Perrone, D., Befus, K. M., et al.: Global aquifers dominated by fossil groundwaters
796 but wells vulnerable to modern contamination, *Nat. Geosci.*, 10, 425–429,
797 <https://doi.org/10.1038/ngeo2943>, 2017.
- 798 Jouzel, J., and Souchez, R. A.: Melting-refreezing at the glacier sole and the isotopic composition
799 of the ice, *J. Glaciol.*, 28, 35–42, <https://doi.org/10.3189/S0022143000011771>, 1982.
- 800 Kim, S., Han, Y., Jung, H., and Lee, J.: Seasonal patterns and diagnostic values of $\delta^2\text{H}$, $\delta^{18}\text{O}$, d-
801 excess, and $\Delta^{17}\text{O}$ in precipitation over Seoul, South Korea (2016–2020), *Earth Syst. Sci.*
802 *Data*, <https://doi.org/10.5194/essd-18-1489-2026>, 2026.
- 803 Kendall, C., and Coplen, T. B.: Distribution of oxygen-18 and deuterium in river waters across the
804 United States, *Hydrol. Process.*, 15, 1363–1393, <https://doi.org/10.1002/hyp.217>, 2001.
- 805 Kendall, C., and McDonnell, J. J. (Eds.): *Isotope Tracers in Catchment Hydrology*, Elsevier,



- 806 Amsterdam, <https://doi.org/10.1016/C2009-0-10239-8>, 1998.
- 807 Levin, N. E., Zipser, E. J., and Cerling, T. E.: Isotopic composition of waters from Ethiopia and Kenya:
808 insights into moisture sources for eastern Africa, *J. Geophys. Res. Atmos.*, 114, D23306,
809 <https://doi.org/10.1029/2009JD012166>, 2009.
- 810 Li, X., Wang, L., Hu, B., Chen, D., and Liu, R.: Contribution of vanishing mountain glaciers to global
811 and regional terrestrial water storage changes, *Front. Earth Sci.*, 11, 1134910,
812 <https://doi.org/10.3389/feart.2023.1134910>, 2023.
- 813 Li, R., Zhu, G., Chen, L., Qi, X., Lu, S., Meng, G., Wang, Y., Li, W., Zheng, Z., Yang, J., and Gun, Y.:
814 Global stable isotope dataset for surface water, *Earth Syst. Sci. Data*, 17, 2135–2145,
815 <https://doi.org/10.5194/essd-17-2135-2025>, 2025.
- 816 Lin, X., Zhu, G., Qiu, D., et al.: Climate and landscape control of runoff stable isotopes in the inland
817 mountain, *J. Hydrol. Reg. Stud.*, 51, 101633, <https://doi.org/10.1016/j.ejrh.2023.101633>,
818 2024.
- 819 Merlivat, L., and Jouzel, J.: Global climatic interpretation of the deuterium–oxygen 18 relationship
820 for precipitation, *J. Geophys. Res.*, 84, 5029–5033,
821 <https://doi.org/10.1029/JC084iC08p05029>, 1979.
- 822 Müller, T., Fischer, M., Lane, S. N., and Schaeffli, B.: Separating snow and ice melt using water
823 stable isotopes and glacio-hydrological modelling, *Cryosphere*, 19, 423–458,
824 <https://doi.org/10.5194/tc-19-423-2025>, 2025.
- 825 NASA JPL: NASA Shuttle Radar Topography Mission Global 1 arc second [data set], NASA LP DAAC,
826 <https://doi.org/10.5067/MEASURES/SRTM/SRTMGL1.003>, 2013.
- 827 Nguyen, C. Q., Kimura, T., and Nakamura, T.: Evaluating mountain recharge in Yamanashi, Japan,
828 using stable isotopes and a hydrogeological groundwater flow model, *Hydrol. Res.*, 56,
829 951–966, <https://doi.org/10.2166/nh.2025.063>, 2025.
- 830 Nicholson, S. E.: A review of climate dynamics and climate variability in Eastern Africa, *Limnol.*
831 *Clim. Paleoclim. East Afr. Lakes*, 25–56, <https://doi.org/10.1201/9780203748978-2>, 2019.
- 832 Ollivier, I., Steen-Larsen, H. C., Stenni, B., et al.: Surface processes and drivers of the snow water
833 stable isotopic composition at Dome C, *Cryosphere*, 19, 173–200,
834 <https://doi.org/10.5194/tc-19-173-2025>, 2025.
- 835 Penna, D., Ahmad, M., Birks, S. J., Bouchaou, L., Brenčić, M., Butt, S., Holko, L., Jeelani, G.,
836 Martínez, D. E., Melikadze, G., Shanley, J. B., Sokratov, S. A., Stadnyk, T., Sugimoto, A., and
837 Vreča, P.: A new method of snowmelt sampling for water stable isotopes, *Hydrol.*
838 *Process.*, 28, 5637–5644, <https://doi.org/10.1002/hyp.10273>, 2014.
- 839 Penn, K., Marshall, S. J., and Sinclair, K. E.: Seasonal enrichment of heavy isotopes in meltwater
840 runoff from Haig Glacier, Canadian Rocky Mountains, *Front. Earth Sci.*, 11, 1125877,
841 <https://doi.org/10.3389/feart.2023.1125877>, 2023.
- 842 Perşoiu, A., Bădăluță, C.-A., and Lee, J.: Stable isotope hydrology of surface and ground waters in
843 King George Island, Antarctica, *Isot. Environ. Health Stud.*, 59, 412–425,
844 <https://doi.org/10.1080/10256016.2023.2281932>, 2023.
- 845 Pesci, M. H., Schulte Overberg, P., Bosshard, T., and Förster, K.: From global glacier modeling to
846 catchment hydrology, *Front. Water*, 5, 1296344,
847 <https://doi.org/10.3389/frwa.2023.1296344>, 2023.
- 848 Popp, A. L., Beria, H., Sprenger, M., Ala-Aho, P., Coenders-Gerrits, M., Groh, J., and Kirchner, J. W.:
849 Recent advances in tracer-aided mixing modeling of water in the Critical Zone, *Rev.*
850 *Geophys.*, 63, e2024RG000866, <https://doi.org/10.1029/2024RG000866>, 2025.
- 851 Pu, T., Chen, P., Wang, S., Shi, X., and Tripathee, L.: Isotopic evolution in snowpacks from a typical
852 temperate glacier in the South-Asia monsoon region, *Water*, 12, 3402,
853 <https://doi.org/10.3390/w12123402>, 2020.



- 854 Rets, E. P., Popovnin, V. V., Toropov, P. A., Smirnov, A. M., Tokarev, I. V., Chizhova, J. N., and
855 Kornilova, E. D.: Djankuat glacier station in the North Caucasus, Russia: a database of
856 glaciological, hydrological, and meteorological observations and stable isotope sampling
857 results during 2007–2017, *Earth Syst. Sci. Data*, 11, 1463–1481,
858 <https://doi.org/10.5194/essd-11-1463-2019>, 2019.
- 859 RGI Consortium: Randolph Glacier Inventory – a dataset of global glacier outlines (version 7), Natl.
860 Snow Ice Data Cent., <https://doi.org/10.5067/F6JMOVY5NAVZ>, 2023.
- 861 Rozanski, K., Araguás-Araguás, L., and Gonfiantini, R.: Isotopic patterns in modern global
862 precipitation, *Geophys. Monogr. Ser.*, 78, 1–36, <https://doi.org/10.1029/GM078p0001>,
863 1993.
- 864 Saidaliyeva, Z., Muccione, V., Shahgedanova, M., Bigler, S., Adler, C., and Yapiyev, V.: Adaptation
865 to climate change in the mountain regions of Central Asia: a systematic literature review,
866 *WIREs Clim. Change*, 15, e891, <https://doi.org/10.1002/wcc.891>, 2024.
- 867 Sharp, M., and Tranter, M.: Glacier biogeochemistry, *Geochem. Perspect.*, 6, 173–339,
868 <https://doi.org/10.7185/geochempersp.6.2>, 2017.
- 869 Shi, X., Risi, C., Pu, T., Lacour, J.-L., Kong, Y., Wang, K., He, Y., and Xia, D.: Variability of isotope
870 composition of precipitation in the Southeastern Tibetan Plateau from the synoptic to
871 seasonal time scale, *J. Geophys. Res. Atmos.*, 125, e2019JD031751,
872 <https://doi.org/10.1029/2019JD031751>, 2020.
- 873 Slemmons, K. E. H., Saros, J. E., and Simon, K.: The influence of glacial meltwater on alpine aquatic
874 ecosystems, *Environ. Sci. Process. Impacts*, 15, 1794–1806,
875 <https://doi.org/10.1039/C3EM00243H>, 2013.
- 876 Sokratov, S. A., and Golubev, V. N.: Snow isotopic content change by sublimation, *J. Glaciol.*, 55,
877 823–828, <https://doi.org/10.3189/002214309790152456>, 2009.
- 878 Staudinger, M., Seeger, S., Herbstritt, B., Stoelzle, M., Seibert, J., Stahl, K., and Weiler, M.: The CH-
879 IRP data set: a decade of fortnightly data on $\delta^2\text{H}$ and $\delta^{18}\text{O}$ in streamflow and
880 precipitation in Switzerland, *Earth Syst. Sci. Data*, 12, 3057–3066,
881 <https://doi.org/10.5194/essd-12-3057-2020>, 2020.
- 882 Stumpp, C., Klaus, J., and Stichler, W.: Analysis of long-term stable isotopic composition in German
883 precipitation, *J. Hydrol.*, 517, 351–361, <https://doi.org/10.1016/j.jhydrol.2014.05.034>,
884 2014.
- 885 Taylor, S., Feng, X., Kirchner, J. W., Osterhuber, R., Klaue, B., and Renshaw, C. E.: Isotopic evolution
886 of a seasonal snowpack and its melt, *Water Resour. Res.*, 37, 759–769,
887 <https://doi.org/10.1029/2000WR900341>, 2001.
- 888 Terzer-Wassmuth, S., Wassenaar, L. I., Welker, J. M., and Araguás-Araguás, L.: Improved high-
889 resolution global and regionalized isoscapes of $\delta^{18}\text{O}$, $\delta^2\text{H}$ and d-excess in precipitation,
890 *Hydrol. Process.*, <https://doi.org/10.1002/hyp.14254>, 2021.
- 891 Thompson, L. G., Mosley-Thompson, E., Davis, M. E., et al.: Tropical glacier and ice core evidence
892 of climate change, *Clim. Change*, 59, 137–155,
893 <https://doi.org/10.1023/A:1024472313775>, 2003.
- 894 Vargas, D., Chimborazo, O., László, E., Temovski, M., and Palcsu, L.: Rainwater isotopic
895 composition in the Ecuadorian Andes and Amazon reflects cross-equatorial flow
896 seasonality, *Water*, 14, 2121, <https://doi.org/10.3390/w14132121>, 2022.
- 897 Vitvar, T., Aggarwal, P. K., and Herczeg, A. L.: Global network is launched to monitor isotopes in
898 rivers, *Eos Trans. AGU*, 88, 325–326, <https://doi.org/10.1029/2007EO330001>, 2007.
- 899 Vital, M., Jara, E., Wade, A., Masse-Dufresne, J., Persoiu, A., Temovski, M., Saidaliyeva, Z.,
900 Shahgedanova, M., Vreča, P., Nishonov, B., Dàvila Roller, L., Lee, J., Fernandoy, F., Pu, T.,
901 Ramirez, E., and Vystavna, Y.: Large-scale isotopic fingerprinting of cryosphere and



- 902 hydrological components in glacierized catchments, Zenodo,
903 <https://doi.org/10.5281/zenodo.19062383>, 2026.
- 904 Viviroli, D., Kumm, M., Meybeck, M., et al.: Increasing dependence of lowland populations on
905 mountain water resources, *Nat. Sustain.*, 3, 917–928, [https://doi.org/10.1038/s41893-](https://doi.org/10.1038/s41893-020-0559-9)
906 [020-0559-9](https://doi.org/10.1038/s41893-020-0559-9), 2020.
- 907 Vodila, G., Palcsu, L., Futó, I., and Szántó, Z.: A 9-year record of stable isotope ratios of
908 precipitation in Eastern Hungary: implications on isotope hydrology and regional
909 palaeoclimatology, *J. Hydrol.*, 400, 144–153,
910 <https://doi.org/10.1016/j.jhydrol.2011.01.030n>, 2011.
- 911 Vreča, P., Bronić, I. K., Horvatinčić, N., and Barešić, J.: Isotopic characteristics of precipitation in
912 Slovenia and Croatia: comparison of continental and maritime stations, *J. Hydrol.*, 330,
913 457–469, <https://doi.org/10.1016/j.jhydrol.2006.04.005>, 2006.
- 914 Vuille, M., Bradley, R. S., and Keimig, F.: Climate variability in the Andes of Ecuador and its relation
915 to tropical Pacific and Atlantic sea surface temperature anomalies, *J. Clim.*, 13, 2520–
916 2535, [https://doi.org/10.1175/1520-0442\(2000\)013<2520:CVITAO>2.0.CO;2](https://doi.org/10.1175/1520-0442(2000)013<2520:CVITAO>2.0.CO;2), 2000.
- 917 Vystavna, Y., Harjung, A., Monteiro, L. R., Matiatos, I., and Wassenaar, L. I.: Stable isotopes in
918 global lakes integrate catchment and climatic controls on evaporation, *Nat. Commun.*, 12,
919 7224, <https://doi.org/10.1038/s41467-021-27569-x>, 2021.
- 920 Vystavna, Y., Chavanne, L., Harjung, A., Soto, D. X., Watson, A., Miller, J., and Cullmann, J.:
921 Predicting river flow dynamics using stable isotopes for better adaptation to climate and
922 land-use changes, *Nat. Water*, 2, 741–748, <https://doi.org/10.1038/s44221-024-00280-z>,
923 2024.
- 924 Woo, M.-K.: *Permafrost Hydrology*, Springer, <https://doi.org/10.1007/978-3-642-23462-0>, 2012.
- 925 Yao, T., Masson-Delmotte, V., Gao, J., et al.: A review of climatic controls on $\delta^{18}\text{O}$ in precipitation
926 over the Tibetan Plateau, *Rev. Geophys.*, 51, 525–548,
927 <https://doi.org/10.1002/rog.20023>, 2013.
- 928 Yang, Y., Wu, Q., Guo, X., Zhou, L., Yao, H., Zhang, D., Zhang, Z., Chen, J., and Liu, G.: First
929 comprehensive stable isotope dataset of diverse water units in a permafrost-dominated
930 catchment on the Qinghai–Tibet Plateau, *Earth Syst. Sci. Data*, 16, 3755–3770,
931 <https://doi.org/10.5194/essd-16-3755-2024>, 2024.
- 932 Yoshimura, K.: Stable water isotopes in climatology, meteorology, and hydrology: a review, *J.*
933 *Meteorol. Soc. Jpn.*, 93, 513–533, <https://doi.org/10.2151/jmsj.2015-036>, 2015.
- 934 Zhang, B., Zang, S., Zhao, L., Wu, X., Liu, R., Dong, X., Yang, D., and Cheng, X.: Characteristics of
935 water stable isotopes and runoff sources of a small permafrost basin in northeastern
936 China, *Front. Earth Sci.*, 12, 1476783, <https://doi.org/10.3389/feart.2024.1476783>, 2024.
- 937 Zhu, G., Liu, Y., Shi, P., Jia, W., Zhou, J., Liu, Y., Ma, X., Pan, H., Zhang, Y., Zhang, Z., Sun, Z., Yong,
938 L., and Zhao, K.: Stable water isotope monitoring network of different water bodies in
939 Shiyang River basin, a typical arid river in China, *Earth Syst. Sci. Data*, 14, 3773–3789,
940 <https://doi.org/10.5194/essd-14-3773-2022>, 2022.